

# Automatic control of output energy in frequency-doubled Nd:YAG laser by close-loop the SHG crystal orientation

A. LAZAR<sup>1,3,\*</sup>, O. DONTU<sup>1</sup>, T. JITSUNO<sup>2,3</sup>

<sup>1</sup>Politehnica University of Bucharest, Bucharest 060042, Romania

<sup>2</sup>Institute of Laser Engineering, Osaka University, Japan

<sup>3</sup>Extreme Light Infrastructure – Nuclear Physics (ELI-NP), Horia Hulubei National Institute for Physics and Nuclear Engineering, Reactorului 30, 077125 Măgurele-Ilfov, Romania

This paper presents a closed-loop energy control system for frequency-doubled Nd:YAG lasers. The automatic energy adjustment was done by changing the second harmonic crystal orientation according to the energy measured by a sensor. An experimental configuration for the output energy stabilization in a low-energy frequency-doubled Nd:YAG laser was designed. An electrically actuated mechanism to rotate the KTP crystal was used to adjust the SHG output energy by changing the angle to the incident laser beam. The shaft of the motor movement is controlled with the electrical signal generated by a minicomputer. The control system was tested at the low energy level in the mJ range and a good control of second harmonic generation was obtained. The output energy was kept at  $3.0 \pm 0.2$  mJ. A short introduction about how frequency-doubled Nd:YAG laser work and its importance of stabilizing output energy are presented.

(Received February 10, 2023; accepted June 6, 2023)

*Keywords:* Frequency-doubled Nd:YAG laser, Second harmonic generation, Automatic control

## 1. Introduction

The continuous development of laser-based systems is taking importance in many fields [1-7]. To improve the emission of laser beams over time, several solutions have been approached. Among the most important contributions we find different automatically controlled system for stabilizing the output power by changing the current and the thermal conversion regime in the nonlinear element [8] and the negative feedback-controlled oscillator [9]. The frequency-doubled Nd:YAG lasers can present instability in energy generated by the aging of the flash lamps or loss of phase matching conditions request for second harmonic generation. Energy fluctuations can also appear due to the temperature drift of the laser system with misalignments of the laser components. The conversion efficiency in the frequency-doubling crystal has a strong dependence on the matching angle to the temperature. The temperature drift of the crystal easily produces the output energy fluctuation.

### 1.1. Motivation

Why energy control is so important for a laser beam? For example, in high-power lasers [10] with frequency-doubled Nd:YAG lasers used in amplification stage, not only the maximum energy is required to achieve the peak

power, but also lower energy is necessary for checking some modules of the system or for their alignment. The system of the automatic control of energy can be useful in the transition from a high power to a low one mode without using additional optical components that can be expensive and time consuming. Frequency-doubled Nd:YAG lasers are used in the amplification of high-power laser pulses, because the wavelength of the generated beam is part of the absorption band of the Ti:Sapphire crystal as in reference [11], after the second harmonic has been generated.

Energy fluctuations of high-power laser affect the parameters of the laser beam in terms of energy, spectral band, and pulse duration. Time stability for these three parameters is one of the criteria that must be mandatory satisfied for a good operation of any high-power laser system from the point of view of the repeatability of the beam from one pulse to another. When there is a variation in the energy of the frequency-doubled Nd:YAG laser (pumping laser) used in the chirped pulse amplification, the peak power of the beam will vary. The pumping laser used to stimulate the fluorescence emission of the Ti:Sapphire crystal must be as stable as possible in energy.

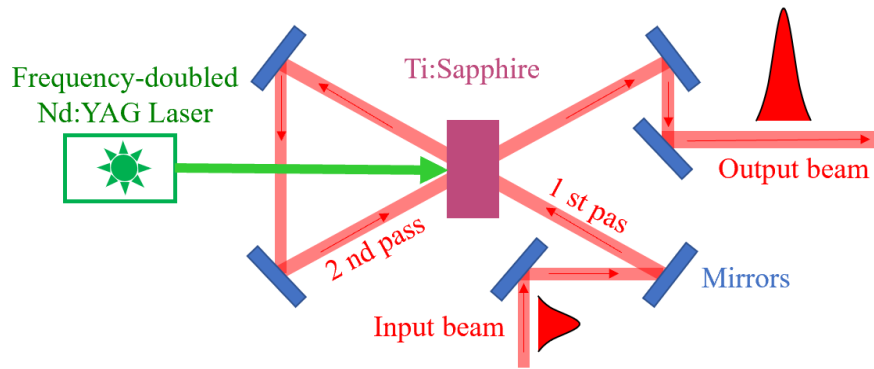


Fig. 1. Example of using the Nd:YAG laser for the amplification of frequency drift laser pulses in an optical configuration with two passes through the Ti:Sapphire crystal. Figure inspired from the reference [12] (color online)

Fig. 1 presents schematically the method by which the process of amplifying high-power laser pulses is done. The beam generated by the frequency-doubled Nd:YAG laser is sent into the Ti:Sapphire crystal to stimulate the population inversion. The laser wavelength is absorbed and converted into energy that will be transferred to the input beam. Each time the beam passes through the crystal, it increases in energy. This is the method of the energy amplification of high-power laser pulses by using frequency-doubled Nd:YAG lasers.

The gain energy ( $G$ ) after amplification can be determined with the formula below. Here fluence is expressed as the ratio between the energy of the laser beam on the surface.  $F_{out}$  is the output fluence and  $F_{in}$  is the input fluence.

$$G = F_{out}/F_{in} \quad (1)$$

## 2. Automatic control energy of the frequency-doubled Nd:YAG laser

### 2.1. How the automatic control of output energy in frequency-doubled Nd:YAG laser works

In this experimental work we propose to maintain a stable output energy of the frequency-doubled Nd:YAG laser [13] by controlling the second harmonic generation (SHG). The laser beam generated by an oscillator laser in infrared (IR) at 1064 nm, will be sent to the surface of the potassium titanyl phosphate (KTP) crystal to get SHG. The KTP crystal will be fixed in a gear mechanism through which the rotational movement from the shaft stepper motor will be transmitted to the crystal. The KTP crystal will be rotated so that the output energy remains stable around a reference value (Fig. 2).

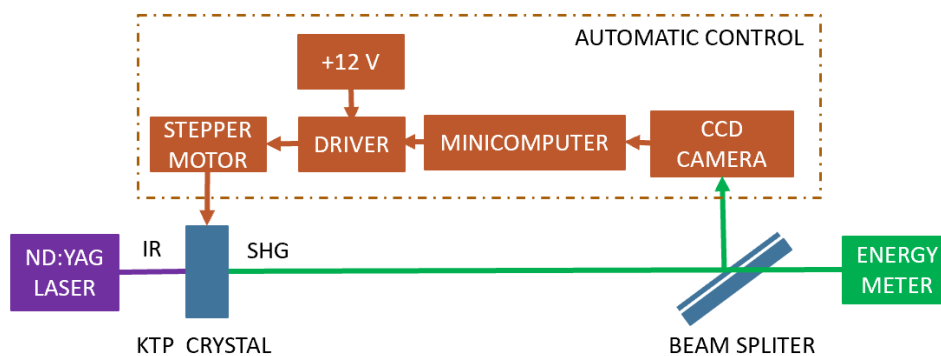


Fig. 2. Close loop control system to maintain a stable output energy of the frequency-doubled Nd:YAG laser by controlling the orientation of KTP crystal (color online)

The energy will be evaluated as a function of the CCD camera pixel intensity produced by the beam intensity. The closed-loop control circuit requires the stepper motor to perform rotational movements according to the values read by the CCD camera. The Raspberry Pi minicomputer will analyze and compare the acquired data with a reference value that corresponds to a certain energy measured with an external energy meter.

The system reference  $r(t)$  is constantly compared by the minicomputer with  $y(t)$  signal provide by the CCD camera (Fig. 3). Under these conditions, the control algorithm must generate the command signal  $u(t)$  to compensate for the energy loss. By changing the orientation angle of the crystal with respect to the beam axis incident on the face of the crystal, the energy will be changed.

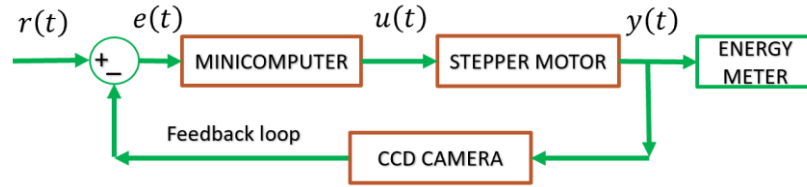


Fig. 3. The basic logic diagram of the control close loop with positive feedback.  $r(t)$  represents the system reference,  $e(t)$  is the calculated error,  $u(t)$  is the control signal and  $y(t)$  is the output or response of the system

The error of the closed-loop system increases according to the following mathematical relationship:

$$e(t) = r(t) - y(t) \quad (2)$$

Generation of the second harmonic is commonly used to convert the wavelength of radiation from Nd:YAG laser to 532 nm, in the middle of the visible spectrum. For this, crystals that can generate the second harmonic are used, such as the KTP crystal [14]. This effect is a 2nd order nonlinear process. To describe more precisely what a nonlinear optical process represents we will consider that the dipole moment per volume unit or the polarization with  $\tilde{P}(t)$ , of a material depends on the strength of the applied electric field  $\tilde{E}(t)$ . In the case of conventional optics, the induced polarization depends linearly on the strength of the electric field described by the following relationship:

$$\tilde{P}(t) = \epsilon_0 \chi^{(1)} \tilde{E}(t) \quad (3)$$

where the proportionality constant  $\chi^{(1)}$  is known as the susceptibility of the medium and  $\epsilon_0$  is the permittivity of free space. In nonlinear optics, the optical response can be described by generalizing the above equation expressing the polarization  $\tilde{P}(t)$ , as a power series in the field intensity  $\tilde{E}(t)$ :

$$\tilde{P}(t) = \epsilon_0 [\chi^{(1)} \tilde{E}(t) + \chi^{(2)} \tilde{E}^2(t) + \chi^{(3)} \tilde{E}^3(t) + \dots] \quad (4)$$

The parameters  $\chi^{(2)}$  and  $\chi^{(3)}$  are known as the susceptibility of nonlinear optics of order 2 and 3. The applied electric field  $\tilde{E}$  is of the order of the intensity of the characteristic atomic electric field  $E_{at} = e/4\pi\epsilon_0 a_0^2$ , where  $e$  is the charge of electron and  $a_0 = 4\pi\epsilon_0 \hbar^2 / m e^2$  is the Bohr radius of the hydrogen atom having Planck's constant divided by  $2\pi$  and  $m$  is the mass of the electron. Numerically we can say that  $E_{at} = 5.14 \times 10^{11} V/m$ . The reason why polarization plays an important role in the description of nonlinear optics phenomena is the fact that the time variation of polarization can act as a source of new components of the electromagnetic field. The laser intensity associated with a strong field of atomic electric field intensity  $E_{at}$  has the following value [15]:

$$I_{at} = \frac{1}{2} \epsilon_0 c E_{at}^2 = 3.5 \times 10^{16} W/cm^2 \quad (5)$$

In an anisotropic medium, for each direction of propagation there are two linear polarization modes for which the polarization is conserved. These waves are orthogonally polarized and propagate at different speeds. In the case of the uniaxial crystal, ordinary and extraordinary waves propagate with refractive indices  $n_o$  and  $n_e(\theta)$  where the angle  $\theta$  defines the direction of wave propagation  $\omega$  in relation to the optical axis. The refractive index  $n_e(\theta)$  varies between  $n_o(\theta = 0^\circ)$  and  $n_e(\theta = 90^\circ)$ . The tensor  $\chi^{(2)}$  gives ordinary and extraordinary waves the possibility to mix in the anisotropic medium. The two waves meet the phase matching conditions for frequency doubling when  $n_e < n_o$ , at the angle value  $\theta_{ap}$  that satisfies the relation  $n_o(\omega) = n_e(2\omega, \theta_{ap})$  and when  $n_e > n_o$ , at the angle value  $\theta_{ap}$  that satisfies the relation  $n_e(\omega, \theta_{ap}) = n_o(2\omega)$  [16].

## 2.2. The schematic of the system and design of the SHG control mechanism

The schematic of the automatic control system of the frequency-doubled Nd:YAG laser is presented in Fig. 4. Nd:YAG is a fundamental laser [17] with four energy levels [18]. Electrons are excited into the photon absorption band by a flash lamp [19]. The role of the resonator is to maintain an electromagnetic field configuration whose losses on the two mirrors are supplemented by the amplification medium through stimulated emission [20]. Photons generated by population inversion are reflected between the low and high reflectivity mirrors of the resonator. When the number of photons in the cavity reaches the maximum value, part of the laser beam is allowed to pass through the mirror with low reflectivity. The laser beam with the wavelength of 1064 nm is sent to the KTP crystal that is fixed in a special mechanism with which the closed-loop phase matching of the incident beam is achieved. After the fundamental beam has been converted to 532 nm, the beam is reflected by the mirrors and is sent to the energy meter. A small reflection from the main beam is reflected by the beam splitter and is sent to the CCD camera which is the feedback element of the system. The beam intensity per pixel is adjusted with attenuation filters.

A detail of the second harmonic crystal orientation mechanism is shown in Fig. 5. The energy control of the laser beam is done by the stepper motor which is commanded by a minicomputer that processes the data

acquired by the CCD camera. Closed-loop control is based on setting a reference that represents the energy value that must be maintained constant during operation. If the value

of the reference energy starts to change, the controller will generate control signals to the driver of the stepper motor that will reposition the crystal to reach the reference.

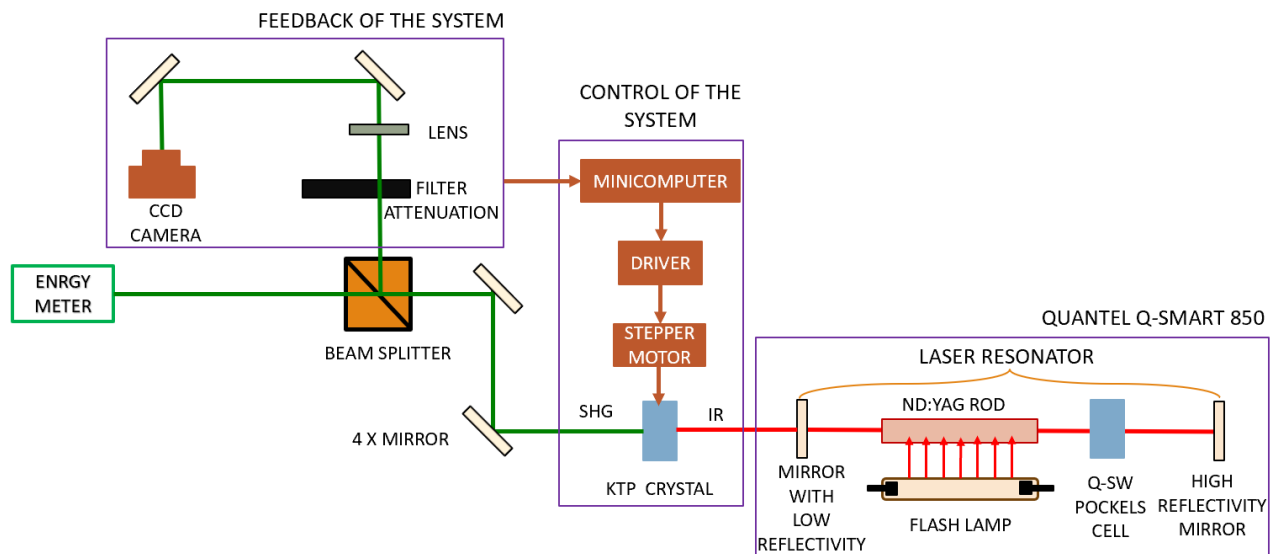


Fig. 4. Scheme of the experimental setup (color online)

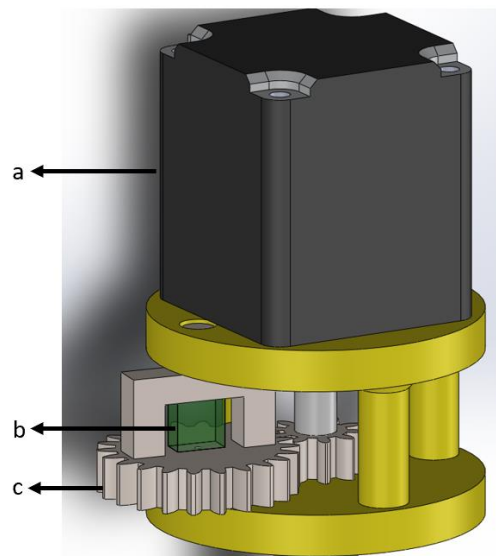


Fig. 5. The design of orientation mechanism of KTP crystal. By driving the stepper motor (a), the gear mechanism (c) will be set in motion, which will rotate the KTP crystal (b) (color online)

### 3. Results and discussion

The output energy control system was assembled and aligned (Fig. 6). Closed-loop control was performed by comparing the pixels of the CCD camera with the reference value. For example, at about 3 mJ of energy (Fig. 7) read by the energy meter, the sum of the pixel intensity of the CCD camera was around 150 (dimensionless). This value was set as the system reference which should ideally remain constant. Once the beam energy starts to vary, the CCD camera will detect

another pixel's intensity value that will be compared to the reference. At this point, if the reading is greater than the set reference, the stepper motor will rotate the crystal in clockwise direction. If the reading is lower than the reference, the motor will rotate the crystal in a counterclockwise direction.

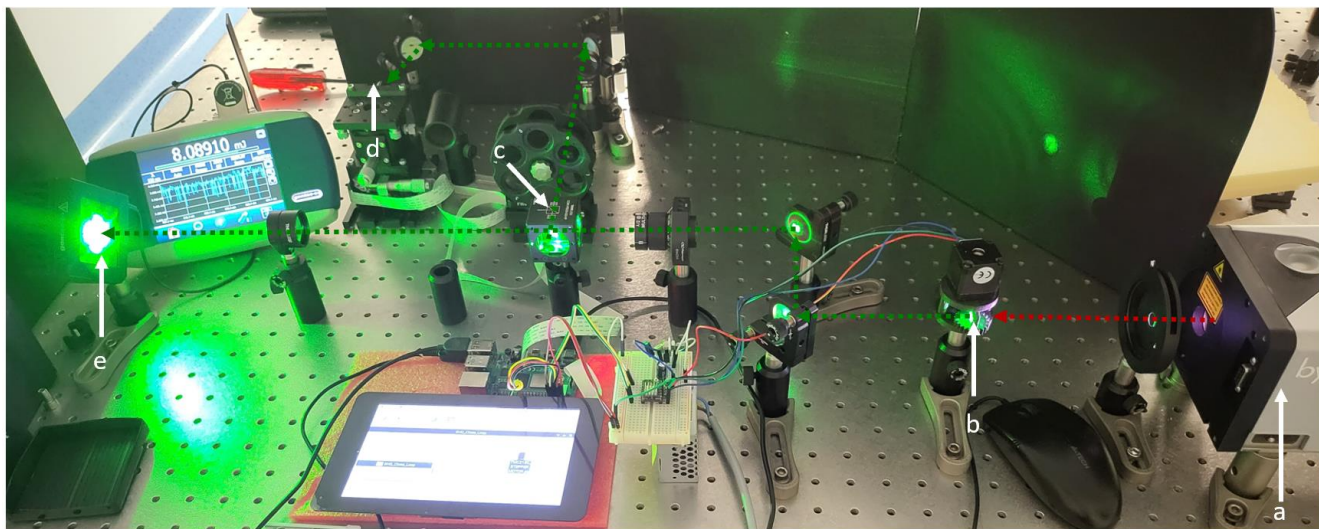


Fig. 6. Experimental configuration. Quantel Q-smart 850 (a) send the laser radiation to the face of the KTP crystal (b) with which the SHG is emitted. The beam emitted at 532 nm is reflected by the mirrors to the energy meter (e). A small part of the beam is reflected by the beam splitter (c) and transmitted to the CCD camera (d) (color online)

The control pulses for the stepper motor are sent via the Raspberry Pi minicomputer. The TMC2130 control driver was used for the voltage and current amplification of the signals from the minicomputer. An external power supply and an electronic voltage stabilizer circuit were used to properly power the motor driver. Some results during the testing of the system are shown in Fig. 7. The control loop algorithms were written in Python and libraries as open-source computer vision library (OpenCV) were used to communicate with the CCD camera. Some of the external pins on the raspberry pi board were used to send and acquire electrical signals. The CCD camera was triggered at 10 Hz with drive signals from the Quantel Q-smart 850 laser oscillator. The CCD camera connects directly to the raspberry pi 3 by way of a 15-pin ribbon cable.

The control system was tested by changing the voltage on the flash lamps of the Quantel Q-smart 850 laser. In Fig. 7 a decrease in energy by 2 mJ is reached when the voltage of the flash lamp drops from 650 V to 600 V. The CCD camera detects a variation of pixel intensity in the 60-65 range. Through the operating conditions of the control algorithms, the minicomputer sends the command signals for the readjustment of the second harmonic emission. From this moment the intensity on the CCD camera gradually increases to the reference. The energy also starts to increase from 1 mJ to 3 mJ. The energy variation around the reference value was in the order of hundreds of  $\mu\text{J}$  conform with measurement plotted in Fig. 7. The output energy stability was  $3.0 \pm 1.0$  mJ without feedback control due to the temperature drift of the crystal, and it was stabilized to  $3.0 \pm 0.2$  mJ with feedback control.

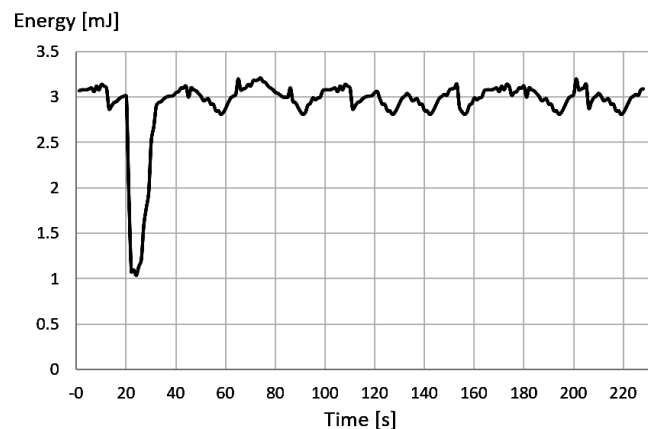


Fig. 7. The energy stability of the control system

#### 4. Conclusions

In this work a closed loop control method of the laser beam energy through the orientation of the SHG crystal was proposed for practical implementation and testing. For practical implementation of the system some components from the design parts were obtained by 3D printing, like CCD camera support, or mechanism to rotate the KTP crystal and so on. For testing the system, beam time at Quantel Q-smart 850 laser from ELI-NP laboratory was requested. After alignment of the optics component, algorithms for camera CCD trigger, pixel value measurements and stepper motor movement were tested.

The energy stability of the laser beam can be optimized by controlling the temperature of the KTP crystal. The crystal orientation mechanism can be improved by replacing the 3D printed components with components made of metallic materials that increase the positioning accuracy. Control algorithms can be simplified

if we use energy measurement tools that are dedicated to the Raspberry Pi minicomputer. Increasing the stability of the control loop can be strengthened by designing an electrically actuated mechanism to rotate the polarization according to the values measured by the sensor. The best system response time can be achieved if piezoelectric actuators are also used in the crystal positioning mechanism. An advanced experimental test can be done by applying the automatic energy control system in high energy lasers, in the range of tens of Joules, which are used in the amplification chain of high-power laser systems. The purpose of this system is to be implemented in frequency-doubled Nd:YAG laser, used in the amplification of ultra-short laser pulses. Using the system in a high-power laser will bring the advantages of reducing the time required to change the energy of the amplified laser pulse and having a stable energy.

### Acknowledgements

This work has been funded by the European Social Fund from the Sectoral Operational Programme Human Capital 2014-2020, through the Financial Agreement with the title "Training of PhD students and postdoctoral researchers in order to acquire applied research skills - SMART", Contract no. 13530/16.06.2022 - SMIS code: 153734.

### References

- [1] A. Popescu, S. Miclos, D. Savastru, R. Savastru, M. Ciobanu, M. Popescu, A. Lőrinczi, F. Sava, A. Velea, F. Jipa, M. Zamfirescu *J. Optoelectron. Adv. M.* **12**, (11), 1874 (2009).
- [2] Y. Li, H. Bai, J. Wu, G. Cao, Y. Zhang, *Optoelectron. Adv. Mat.* **16**(11-12), 545 (2022).
- [3] Y. Sun, Y. Xu, *J. Optoelectron. Adv. M.* **24**(7-8), 332 (2022).
- [4] D. Gandhi, S. Gupta, *J. Optoelectron. Adv. M.* **24**(7-8), 304 (2022).
- [5] M. K. Ikhwan, M. F. A. Rahman, M. H. Fatheli, F. S. M. Sammsamnun, H. Haroon, A. A. Latiff, *J. Optoelectron. Adv. M.* **23**(7-8), 307 (2021).
- [6] S. K. Liaw, D. C. Li, Y. L. Yu, H. W. Chen, H. C. Lee, H. H. Tsai, *J. Optoelectron. Adv. M.* **23**(3-4), 97 (2021).
- [7] I. Avarvarei, O. Dontu, J. L. Ocana, D. Savastru, T. Prisecaru, R. Ciobanu, D. Besnea, *The Romanian Review Precision Mechanics, Optics & Mechatronics* **41**, 179 (2012).
- [8] A. Simonov, V. Shmalgauzen, O. Myzin, *J. Quantum Electronics* **27**(9), 805 (1997).
- [9] P. Yankov, G. Petrov, *APPL PHYS B Photophysics and Laser Chemistry* **54**(3), 231 (1992).
- [10] W. Li, Z. Gan, L. Yu, *Optics Letters* **43**(22), 5681 (2018).
- [11] J. Dong, P. Deng, *J. Cryst. Growth*, **261**(4), 514 (2003).
- [12] R. Dabu, *Crystals* **9**(7), 347 (2019).
- [13] B. M. Walsh, *Opt. Mater.* **65**, 2 (2017).
- [14] K. Kato, *IEEE J. Quantum Electronics*, **28**(10), 1974 (1992).
- [15] L. K. Chen, W. R. Bosenberg, C. L. Tang, *Prog. Cryst. Growth Charact. Mater.* **20**, 9 (1990).
- [16] R. W. Boyd, "Nonlinear optics", Third Edition, Elsevier, Rochester, New York (2007).
- [17] H. Y. Zhu, C. W. Xu, J. Zhang, D. Y. Tang, D. W. Luo, Y. M. Duan, *Laser Phys. Lett.* **10**(7), 075802 (2013).
- [18] H. Okada, K. Sumimura, H. Yoshida, H. Fujita, M. Nakatuska, *Quantum Electron. Laser Sci. Conf.* (2005).
- [19] S. Kostic, Z. Ž. Lazarevi, V. Radojevic, A. Milutinovic, M. Romcevic, N. Ž. Romcevic, *Mater. Res. Bull.* **63**, 80 (2015).
- [20] A. Mamrashev, N. Nikolaev, *Crystals* **8**(8), 310 (2018).

\*Corresponding author: lazar.alexandr@yaho.com